Translational Oncology 14 (2021) 100911

Contents lists available at ScienceDirect

Translational Oncology

journal homepage: www.elsevier.com/locate/tranon

The tumor microenvironment may trigger lymphoproliferation in cardiac myxoma

Eugeniu Jantuan[a], Brian Chiu[a,1], Bonnie Chiu[a], Fan Shen[a], Gavin Y Oudit[b], Consolato Sergi[a,c,d,e,1,*]

[a] Department of Laboratory Medicine and Pathology, University of Alberta Hospital, 8440-112 Street, Edmonton T6G 2B7, Alberta, Canada
[b] Department of Medicine, Division of Cardiology, Mazankowski Alberta Heart Institute, Edmonton, AB, Canada
[c] Department of Pediatrics, Faculty of Medicine and Dentistry, University of Alberta, Edmonton, AB, Canada
[d] National "111" Center for Cellular Regulation and Molecular Pharmaceutics, Key Laboratory of Fermentation Engineering, Hubei University of Technology, Wuhan, Hubei, China
[e] Tianyou Hospital, Wuhan University of Science and Technology, Wuhan, Hubei, China

ARTICLE INFO

Keywords:
Cardiac myxoma
Tumor microenvironment
Autophagy
Autophagy-inflammation interplay
Lymphoproliferative disorder

ABSTRACT

Cardiac myxomas (CM) and primary cardiac lymphoproliferative disorders (LPD) are rare primary cardiac neoplasms. The composite occurrence of LPD in CM has been occasionally reported, and chronic inflammation in response to viral infection has been suggested to be at the basis of oncogenesis. Cancers can upregulate autophagy to endure microenvironmental stress and to increase local growth and aggressiveness. CM exhibit a dichotomous separation in low and high inflammatory grades (LIG vs. HIG). We studied 23 CMs using autophagy-related proteins and NanoString technology for gene expression. Autophagy-related proteins (Beclin-1, LAMP-1, LC3, and p62) were demonstrated in both tumor and stromal cells. *ATG* genes showed a progression of involvement in CM using an 8-gene signature. They were associated with Epstein-Barr virus (EBV) encoded latent membrane protein 1 (EBV LMP1) activation. We suggest that CM can upregulate autophagy, creating a favorable environment for EBV-driven oncogenesis. To the best of our knowledge, the present study is the first to report on the TME using the expression of autophagy-related genes and proteins in CM. The microenvironment of CM is dynamic, with a variety of cell types and different molecular pathways at play, and this study may clearly warrant further investigation.

Introduction

Cardiac myxoma (CM) is the most common primary cardiac tumor [1–4,5]. Lepidic cells in a sparsely cellular myxoid stroma with cord-like, pseudo-vascular, or vasoformative growth patterns characterize this tumor [4]. Chronic inflammation, fibroblastic proliferation, dystrophic calcification, and even ossification within the CM have also been described [4]. These tumors are histologically benign, slow-growing neoplasms of unclear histogenesis, but may be associated with heart failure and/or cardiac arrhythmias [6–9]. They are most commonly sporadic, but up to 10% are associated with the Carney complex with a familial inheritance pattern [10–13]. Viral histogenesis has recently been entertained in some studies [14,15], but refuted by others [16–18]. Lymphoproliferative disorders (LPD) primarily involving the heart (primary cardiac lymphoma/lymphoproliferative disorders PC-LPD) are infrequent [19], and such tumors arising in CM as composite tumors are unique.

Interestingly, all LPD were found incidentally on microscopic examination of excised CM specimens [19–22] (**Supplemental Table 1**). Lymphomas of B-cell phenotype may indeed co-exist with CM, the majority of which are diffuse large B-cell lymphoma (DLBCL). In up to 4/5 of patients, Epstein-Barr virus (EBV) infection can be detected. Despite the central nervous system (CNS) involvement due to tumor embolization [21], these patients usually present with clinical-stage 1E (localized involvement of a single extra lymphatic/extranodal myxoma) [19]. These patients with post-surgical resection of the LPD arising in CM (LPD-CM) with or without chemotherapy or radiation therapy, on follow-up periods ranging from 3 months to 10 years, exhibit no evidence of lymphoma recurrence or dissemination [19,20,23].

The pathogenetic mechanism of LPD-CM has not been substantially elucidated, but some dysregulation of the immune surveillance has been occasionally postulated [19,20,23]. The association of DLBCL with EBV infection but without underlying systemic immunosuppression may suggest an age-related decline of adaptive immunity or immune senes-

* Corresponding author at: Department of Laboratory Medicine and Pathology, University of Alberta Hospital, 8440-112 Street, Edmonton T6G 2B7, Alberta, Canada.
E-mail address: sergi@ualberta.ca (C. Sergi).
[1] Both authors contributed equally to the preparation of the manuscript.

https://doi.org/10.1016/j.tranon.2020.100911
Received 14 August 2020; Received in revised form 2 October 2020; Accepted 5 October 2020

cence, and an EBV has driven LPD transformation in a cytokine-rich milieu of a CM [20]. The presence of chronic inflammatory foci in LPD-CM is further supportive of the mechanistic explanation of local production of cytokines in stimulating the development of LPD associated with chronic inflammation [20,24]. Restriction of tumor cell proliferation to the CM environment with no evidence of lymphoma recurrence or dissemination is also intriguing. CM may create an enclosed microenvironment permitting accumulation of cytokines and EBV-infected B-cells that can evade T-cell immunosurveillance [21,25–27].

It is now well established that neoplasms co-evolve with the tumor microenvironment (TME) [28]. The TME includes stromal cells, including vasculature, fibroblasts, adipocytes, and different subsets of immune cells. It plays a crucial role in carcinogenesis, cancer progression, dissemination, and resistance to therapy [29,30]. There is a growing body of evidence to suggest that autophagy is a vital regulator of the TME and regulating tumor immunity [28,29,31,32]. The multifaceted role of autophagy in the complex cancer TME depends on a specific context. Autophagy may function as a tumor-suppressive mechanism during early tumorigenesis by the elimination of unhealthy intracellular components and proteins, and regulates antigen presentation to and by immune cells supporting anticancer immune response [29,31]. Dysregulation of autophagy is likely to contribute to tumor progression by promoting genome damage and instability, and autophagy in stromal cells supplying nutrients to cancer cells may fuel cancer growth in established tumors [31,33]. Cancers can upregulate autophagy to endure microenvironmental stress and to increase local growth and aggressiveness.

Autophagy is an evolutionarily conserved intracellular process that enables the degradation and recycling of long-lived large molecules or damaged organelles using the lysosomal-mediated pathway [34–38]. Autophagy occurs constitutively at low basal levels and in the maintenance of normal cellular homeostasis but is induced in response to many types of stress [36,39]. Autophagy dysregulation has been linked to the development of heart failure, infection, tumorigenesis, neurodegeneration, and aging [32,34,36,37]. The molecular mechanisms of autophagy have been extensively reviewed, and the TME can be investigated targeting autophagy [28,34,35,37]. The induction of autophagy results in the recruitment of autophagy-related proteins (ATG) and isolation membranes to form a cup-shaped structure called the phagophore [35]. Expansion and sealing of the phagophore form a double-membrane vesicle termed the autophagosome. Delivery along microtubules to lysosome and fusion of their outer membranes form an autolysosome. Autophagy can be induced by different kinds of stress, including infection, inflammation, nutrient deprivation, and hypoxia. More than 30 ATG genes have been involved in the autophagy process [38].

In this study, we aimed to assess the TME in cardiac myxomas. The NanoString ® gene expression platform was used for gene expression studies. NanoString is a digital counting technology without any enzymatic reactions and accurate for quantifying linear mRNAs. This method is suitable for analyzing highly degraded RNA isolated from formalin-fixed paraffin-embedded (FFPE) tissues that are routinely stored in pathology departments as the probes target short RNA-sequences, and no reverse transcription (RT) or amplification steps are involved. Therefore, NanoString ® technology is not prone to artifacts and bias associated with RT and PCR amplification [40].

Materials and methods

Archival CM cases and histopathology. Twenty-eight formalin-fixed and paraffin-embedded (FFPE) human cardiac myxomas were retrieved from files of the University of Alberta Hospital over six years, 2010–2016, and were used for this study. The ethics committee of the University of Alberta (Edmonton, Canada) approved the study (REB Approval no. Pro00057260). We used serial deparaffinated sections (4 μm-thick) for staining procedures, including hematoxylin and eosin (H&E) and immunohistochemistry. On H&E sections, components of CM-TME were identified, and chronic inflammation was graded as low- and high-inflammatory grade (LIG, HIG).

Immunohistochemistry. Four-μm thick sections were obtained from each FFPE tissue block. The sections were placed on Aptex glass slides, dewaxed and rehydrated in a graded alcohol series, and stained using the streptavidin-biotin-peroxidase complex method and counterstained according to manufacturers' protocols. A mediastinal lymph node was used as a positive control for autophagy markers. A negative control slide was included in each immunostaining. The primary antibody replaced by the same isotype (IgG) antibody, targeting different antigens. We used the following antibodies 1. Autophagy markers: rabbit polyclonal anti – Beclin 1 (ab55878, 1:200 dilution; Abcam), rabbit polyclonal anti – LAMP 1 (ab24170, 1:1000 dilution; Abcam), rabbit polyclonal anti - LC3B (ab63817, 1:200 dilution; Abcam), SQSTM1/p62 (ab56416 at 1:1000 dilution, Abcam), 2. Myxoma cell markers: CD31, CD34, Calretinin, negative markers: smooth muscle (SM) actin, S100 and vimentin, and 3. Inflammatory cells and lymphoma markers: CD3 (T-cell), CD68 (macrophages), CD45 (leukocyte common antigen), CD20, PAX5, BCl2, BCL6, c-Myc, Ki67(MIB1), CD10, and CD5. 4. Viral markers: HSV1, HSV2, LMP1 (EBV), and EBER by in-situ hybridization (ISH).

Immunostaining results were evaluated, graded, and scored by extent (0 = none, 1 = 1–25%, 2 = 26–50%, 3 = 51–75%, 4 = 76–100% of the myxoma cells) and intensity (0 = negative, 1 = weak, 2 = moderate, and 3 = intense). An immunohistochemical score was calculated for each case in which the percentage of positive rating was multiplied by the intensity rating. The immunostaining was judged to be antibody-specific by following two criteria: staining use of normal serum produced no consistent immunostaining of any cells and signal intensity diminished as the dilution of antibody was increased.

Gene expression

Twenty-three CM blocks were selected for RNA extraction and gene expression analysis. Three successive 20-μm thick sections were obtained from each FFPE tissue block. RNA was obtained with RNeasy FFPE Kit (Qiagen, Toronto, ON), and its concentration and purity were studied with the NanoDrop 2000c spectrophotometer (Thermo Fischer Scientific, Waltham, MA). Oligonucleotide probes were produced for the following human genes: *ATG9A, ATG12, ATG14, BECN1, EBV LMP1, LAMP1, MAP1LC3, SQSTM1*, and *WIPI1* (Integrated DNA Technologies, Coralville, IA) (Table 1). For data normalization, three housekeeping human genes were included in the study: *GAPDH, HPRT1*, and *TBP*. Gene expression was quantified with NanoString nCounter platform as per manufacturer recommendations (Nanostring Technologies, Seattle, WA). In detail, with regard to the code set design, a literature search was performed to identify genes involved in autophagy-related cancer biology. The genes selected as a result included three housekeeping genes: *GAPDH, HPRT1*, and *TBP*. Custom nCounter probes for the gene set were designed by NanoString Technologies and manufactured by Integrated DNA Technologies [Coralville, IA, U.S.A.]. Details of the nCounter technology have been reported previously in a report on thyroid cancer by our University [41]. Briefly, a custom nCounter code set consisting of multiplexed probes targeting the gene set was used for gene expression analysis. Each code set included selected housekeeping genes to control for variations in RNA input and quality. Probe pairs with sequences specific to a 100-base region of each target messenger rna were designed using a 3′ biotinylated capture probe and a 5′ reporter probe tagged with a specific fluorescent barcode, thus creating 2 sequence-specific probes for each target transcript. Probes were hybridized with rna at 65 °C and then applied to the nCounter Preparation Station for automated removal of excess probe and immobilization of probe-transcript complexes on a streptavidin-coated cartridge. Data were collected using the nCounter Digital Analyzer by counting the individual barcodes. Raw gene expression counts were quality-controlled and normalized using the nSolver Analysis Software

Table 1
Autophagy-related 8-gene Set (red), EBV LMP-1 (blue), and three housekeeping genes (black).

Gene	Gene name	Functional association
ATG12	Autophagy related protein 12	Autophagosome formation
ATG14	Autophagy related protein 14	Beclin 1 – associated autophagy-related key regulator
ATG9A	Autophagy-related protein 9A	Autophagy
BECN1	Beclin-1	Autophagosome formation
LAMP1	Lysosomal associated membrane protein 1	Lysosomal associated autophagy
MAP1LC3B	Microtubule associated protein 1 light chain beta	Autophagosome formation
SQSTM1	Sequestosome 1/ubiquitin-binding protein p62	Autophagosome cargo protein that targets proteins for selective autophagy
WIPI1	WD repeat domain, phosphoinositide interacting 1	Early autophagosome formation
EBV LMP1	Epstein-Barr virus-encoded latent membrane protein 1	EBV oncoprotein, tumor necrosis factor homologue
GAPDH	Glyceraldehyde-3-phosphate dehydrogenase	Housekeeping
HPRT1	Hypoxanthine phosphoribosyl transferase 1	Housekeeping
TBP	TATA box binding protein	Housekeeping

(version 4.0: NanoString Technologies) and manufacturer-included positive and negative controls. Quality control (qc) parameters include imaging qc, binding density qc, overall assay efficiency, assay linearity, and limit of detection. Data were normalized to the three housekeeping genes to correct for variation in rna input quantity.

Statistics

Normalized transcript counts were used for individual gene analysis. Differential gene expression was assessed using Student's *t*-test. Statistical significance was considered at $P < 0.05$. SPSS version 26 was used.

Results

Histopathology

Histologically, the CM exhibit unique heterogeneous features with myxoma cells scattered in a myxoid stroma. The tumor cells are in single cells, cord-like, pseudo-vascular or vasoformative patterns [42]. The spindle tumor cells without significant atypia surround small blood vessels and scattered lymphoplasmacytic, histiocytic cells, and fibroblastic cells in the myxoma tumor microenvironment (Fig. 1). The inflammatory infiltration was graded: LIG ($N = 12$) and HIG ($N = 11$). Two cases of lymphoproliferative disorders arising within CM were encountered in our series: chronic lymphocytic leukemia (CLL) and DLBCL.

Immunohistochemistry

i) Cardiac myxoma. Myxoma cells were immune-positive for calretinin, vimentin, CD31, CD34, but negative for SM actin or S100.
ii) Autophagy: LAMP 1, Beclin-1, LC3 were strongly immune-positive in the majority of cases (70–92.3%). Nine instances of CM have stained additionally for the SQSTM1/p62 marker. All these cases (100%) express the marker with weak to moderate intensity (1 to 2+). Inflammatory cells and vascular cells stained less intensely. CM with DLBCL was negative for the LC3 marker. However, it expressed a robust Beclin-1 intensity (3+) (Fig. 2).
iii) Inflammatory cells, LPD, and autophagy: Mixed T-cells, B-cells, and macrophages were seen in the inflammatory infiltrates. Both LPD were confirmed with lymphoma markers as CLL/SLL and high-grade B-cell lymphoma (HG-BCL: MYC and BCL2 rearrangement). Beclin1 and p62 were strongly positive, LAMP1 focally and LC3 only rare cells were immune-positive (Figs. 2 and 3).
iv) Viral markers: In CLL/SLL, EBV by LMP1 staining was positive, but EBER by ISH was negative. In HG-BCL, EBV-ISH was positive. In selected cases, HSV1 and HSV2 staining was negative.

ATG gene expression

i) RNA and quality control

Mean RNA yield for 23 FFPE samples was 68.2 ± 60.3 (mean ± SD) ng/μL (range 13.4–312.2 ng/μL) with a mean A260/A280 RNA purity ratio of 1.85 ± 0.07 (1.71–1.96). One case (1/24) was excluded from the study due to low 260/280 ratio (1.42). No significant quality control or normalization issues were encountered. However, 2/8 genes (25%) demonstrated very low counts (close to negative controls) across all samples and were excluded from subsequent analysis: EBV LMP1 (2.9 ± 3.7) and ATG12 (7.4 ± 3.9). ii) All ATG genes were expressed in CM with marked accumulation of SQSTM1/p62, which was 2.5 to 46 folds higher than the remaining ATG genes. When HIG to LIG groups were compared, the HIG group was trending lower, and both MAP1/LC3B and WIPI1 were statistically significant with *p*-value <0.05 using the Student's *t*-test (Table 2) Both LC3B and WIPI1 were associated with autophagosome formation [43].

Discussion

Our study confirms that the CM tumor microenvironment (CM-TME) is very complex and dynamic. CM-TME consists of a variety of intrinsic and extrinsic cells and factors/elements: tumor cells, stromal and vascular cells, inflammatory cells, and infective components/organisms with multiple molecular pathways at play. These processes and events are expected as the CM are exposed continuously to circulating cellular or non-cellular elements and extrinsic elements, including infective organisms/factors [26,27,44,45]. LAMP 1, Beclin-1, LC3 were strongly immune-positive in the majority of cases and nine CMs demonstrated an additional expression of the SQSTM1/p62 marker. All these cases expressed this marker with weak to moderate intensity, while inflammatory cells and vascular cells stained less intensely. As indicated above, CM with DLBCL was negative for the LC3 marker, but it expressed strongly Beclin-1 intensity (3+). Mixed T-cells, B-cells, and macrophages were seen in the inflammatory infiltrates and both LPD were confirmed with lymphoma markers as CLL/SLL and high-grade B-cell lymphoma (HG-BCL with *MYC* and *BCL2* rearrangement). Here, both Beclin1 and

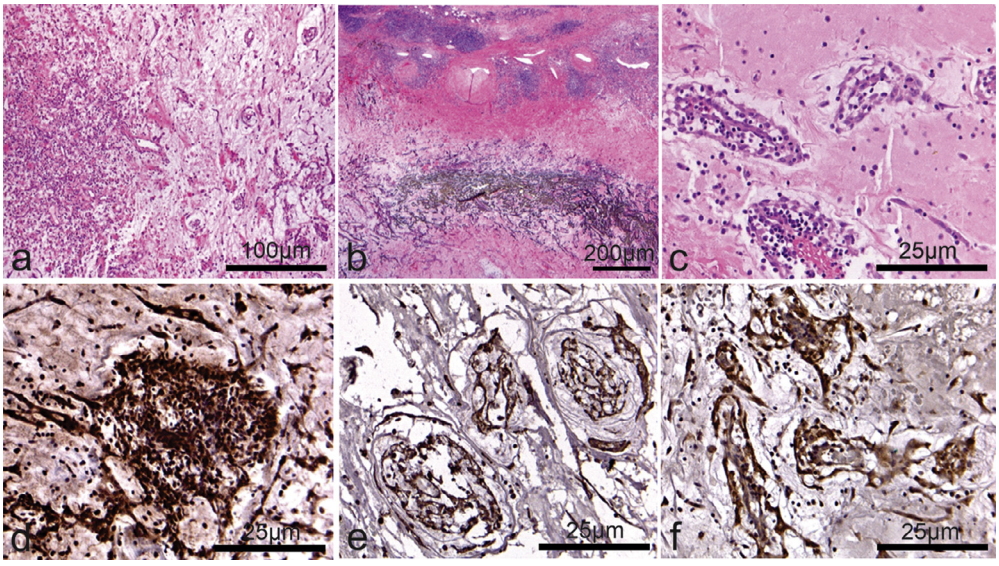

Fig. 1. (a) Cardiac myxoma with chronic inflammation. Magnification 100x. (b) Cardiac myxoma with high inflammatory grade (HIG) and Gamna-Gandy bodies. Magnification 20X. (c) Cardiac myxoma with sparse or low inflammatory grade (LIG). Magnification 200X. 2D – 2F Cardiac myxoma cells in vasoformative patterns with autophagy markers with immunohistochemical positivity in myxoma and stromal cells (2D- LC3), (2E-LAMP1), (2F-p62). Magnification 200x.

Table 2
Autophagy gene expression.

										t-Test		
ATG genes			LIG				HIG			p-value		
ATG14			113				119			0.397		
ATG9A			126				122			0.364		
BECN1			228				211			0.079		
LAMP1			1031				928			0.108		
MAP1LC3B			230				195			0.014		
SQSTM1			2630				2454			0.273		
WIPI1			62				48			0.031		
LIG CM Cases												
ATG14	148.7	153.35	142.71	79.27	67.16	122.52	60.53	108.24	134.89	88.6	139.99	112.96
ATG9A	131.71	97.59	129.43	113.24	109.27	211.63	120.11	103.91	127.18	160.49	87.11	124.08
BECN1	229.43	181.23	212.4	249.12	217.41	243.45	204.66	279.97	244.73	225.3	240.32	209.63
LAMP1	1062.17	947.97	1045.43	832.29	824.1	946.74	1159.74	1597.59	990.47	867.27	1236.62	866.68
MAP1LC3B	152.95	195.17	262.19	249.12	211.72	294.37	264.23	264.1	216.78	250.61	199.1	198.52
SQSTM1	3305.49	4433.15	2170.5	1862.73	1950.97	3335.09	3012.25	2107.03	2900.1	2176.54	1920.26	2386.69
WIPI1	97.72	27.88	89.61	73.6	64.88	62.06	59.57	63.5	55.88	69.36	42.78	35.19
HIG CM Cases												
ATG14	124.59	130.1	123.01	158.58	127.41	67.26	114.17	121.98	118.54	112.31	113.76	
ATG9A	179.97	89.02	129.28	137.15	98.91	93.75	122.54	98.41	115.83	119.23	156.43	
BECN1	207.66	208.85	199.01	295.73	209.55	172.22	216.43	195.05	199.83	204.39	210.37	
LAMP1	1024.43	1013.44	763.12	792.91	1047.76	897.8	1306.51	872.13	975.43	735.33	774.29	
MAP1LC3B	263.03	190.02	149.65	188.58	196.14	195.66	201.88	156.75	179.51	204.66	218.7	
SQSTM1	3502.45	2285.37	3249.92	2944.47	2673.88	1806.8	2428.33	1780.2	2326.12	1754.09	2243.91	
WIPI1	55.37	41.09	74.43	30	33.53	58.09	40.11	55.39	50.13	40.98	48.55	

Notes: CM, cardiac myxoma; LIG, lower inflammation grade; HIG, high inflammation grade.

p62 were strongly positive, while LAMP1 was focally positive and LC3 was positive in only very few cells.

Consistent with the immunohistochemical results of positive autophagy activity, all autophagy-related genes were expressed in the LIG and HIG groups. It seems that all steps in the autophagy process are active. However, there is marked p62 excessive expression (ranging from 2.5 to 46 folder increase compared with the other ATG studied). Further, p62 accumulates when autophagy is inhibited, and aberrant excessive p62 accumulation may result from autophagy defect, causing oxidative stress and has been linked to tumorigenesis [46,47]. Autophagy gene expressions are trending lower in high inflammatory grades than low inflammatory grade with LC3 and WIPI1, achieving statistical significance (p <0.05), further suggesting that autophagosome formation is at reduced levels with a high inflammatory degree.

Viral histogenesis has been postulated in both CM and LPD in cardiac myxomas. The detection of herpesviruses (HSV1 and HSV2) and chronic inflammation in CM suggest a pathogenetic role in the tumor development [14,15]. However, other studies have found neither such association nor a detectable HSV viral protein or genomic DNA by both immunohistochemistry and polymerase chain reaction [16–18]. Our study also detected no evidence of HSV infection, but EBV-LMP1 was detected in CLL-CM, and EBV-ISH was positive in HG-BCL. In “pre”-lymphomatous CM tissues, EBV-LPM1 gene expression was negative.

The above data suggest that the TME with a reduction of gene expression for autophagosome formation and aberrant excessive p62 accumulation in the presence of high inflammatory grade and perhaps viral infection may support the development of lymphoproliferative disorders. To the best of our knowledge, the present study is the first to report on the TME using the expression of autophagy-related genes and proteins in CM.

Our study on CM-TME with ATG-inflammation interplay has some limitations. This study is a single-center retrospective study with a limited but well-characterized number (n = 28) of patients. Although

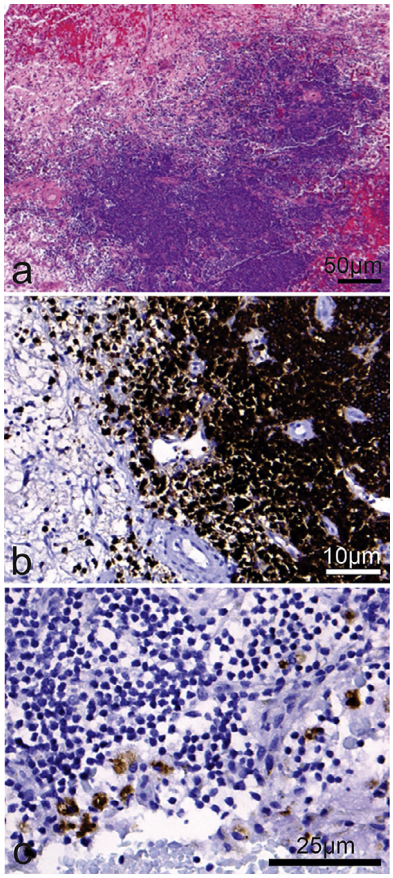

Fig. 2. A Cardiac myxoma-with chronic lymphocytic leukemia (CLL/SLL). Magnification 50x. B. CLL – immunopositive for B-cells/ CD20. Magnification 200X. C. CLL – immunopositive for EBV-LMP1. Magnification 400X.

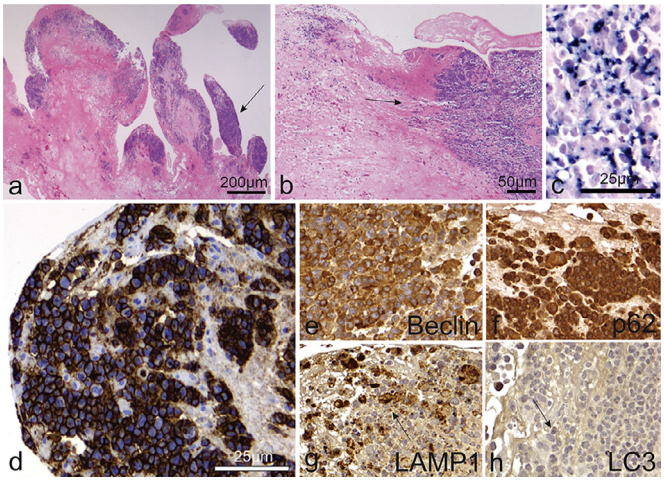

Fig. 3. A-B Cardiac myxoma- with high-grade B-cell lymphoma (HG-BCL). Magnification 20x, 50X. C EBV-ISH positive staining. D HG-BCL Strongly immunopositive for B-cell/CD20. E-H Composite of autophagy markers with BCLN1 and p62 strongly positive, and EBV-LAMP1 patchy positive, and LC3 with rare positive cells. 3C-3E. Magnification 400x.

the selection of specific areas with inflammation can theoretically lead to selection bias and depends on the number of tumor sections examined, quality controls were carried out for all tissue sections with optimal inter- and intraindividual *k* values. Immunohistochemical staining identified autophagic activity is present in all cell types, including CM cells. At the same time, Nanostring assay confirmed overall *ATG* gene expression activity, without identification of such events in specific cell types. The molecular machinery of autophagy is extraordinarily dynamic. Static analyses cannot distinguish between autophagy upregulation and degradation inhibition at a certain stage of the autophagic process. The mechanism underlying how autophagy proteins influence the TME in CM remains to be fully elucidated. Future studies may include in vivo research of a tumor, which may behave similarly as CM. More ATG genes relevant in the autophagy process to identify autophagy upregulation and degradation inhibition at a particular stage of the autophagic process may be highly relevant. The inclusion of inflammatory elements, including inflammasome and inflammatory cytokines, may elucidate the autophagy-inflammation interplay in the CM-TME as previously suggested in targeting NLRP3 inflammasome and currently for SARS-CoV-2 infection [48,49]. Intracardiac myxoma localization and restriction of LPD proliferation within the CM-TME environment is also intriguing and further studies on subsets of immune cells in CM-TME may shed some light on immune-evasion. The concept of tumor microenvironment includes many actors (cellular and acellular) and different conditions (stiffness, architecture) and we particularly focused on autophagy and viral infection. We are completely aware that our data should be correlated with other microenvironmental markers and the extracellular matrix components are usually involved in autophagy regulation as well as the deposition of integrin in the extracellular matrix, which will be the object of future studies.

In conclusion, we report for the first time on the TME using the expression of autophagy-related genes and proteins in CM and these data will be an avenue for further investigating the intriguing relationship between virus infection and cancer.

Declaration of Competing Interest

All authors have nothing to disclose with regard to any financial and personal relationships with other people or organizations that could inappropriately influence (bias) their work.

CRediT authorship contribution statement

Eugeniu Jantuan: Data curation, Writing - original draft, Writing - review & editing. **Brian Chiu:** Conceptualization, Data curation, Writing - review & editing, Formal analysis. **Bonnie Chiu:** Data curation, Writing - review & editing. **Fan Shen:** Writing - review & editing. **Gavin Y Oudit:** Writing - review & editing. **Consolato Sergi:** Conceptualization, Data curation, Writing - review & editing.

Acknowledgments

We are very grateful to Dr. B. Adam for the analysis and interpretation of the NanoString results. This research has been funded by the generosity of the Stollery Children's Hospital Foundation and supporters of the Lois Hole Hospital for Women through the Women and Children's Health Research Institute (WCHRI, Grant ID #: 2096) and Hubei Province Natural Science Funding for Hubei University of Technology (100-Talent Grant for Recruitment Program of Foreign Experts Total Funding). The funders had no role in study design, data collection, and analysis, decision to publish, or preparation of the manuscript.

Supplementary materials

Supplementary material associated with this article can be found, in the online version, at doi:10.1016/j.tranon.2020.100911.

References

[1] F. Fernandes, H. S., B.M. Ianni, E. Arteaga, F.J. Ramires, C. Mady, Primary neoplasms of the heart. Clinical and histological presentation of 50 cases, Arq. Bras. Cardiol. 76 (2001) 231–237.

[2] B, M.A. Obrenović-Kirćanski, B. Parapid, P. Djukić, V. Kanjuh, N. Milić, N. Kovačević-Kostić, M. Velinović, P. Seferović, M. Vraneš, A 30-year-single-center experience in atrial myxomas: from presentation to treatment and prognosis, Thorac. Cardiovasc. Surg. 61 (2013) 530–536, doi:10.1055/s-0032-1322545.

[3] J.G. Wang, B. W., Y. Hu, J.H. Liu, B. Liu, H. Liu, P. Zhao, L. Zhang, Y.J. Li, Clinicopathologic features and outcomes of primary cardiac tumors: a 16-year-experience with 212 patients at a Chinese medical center, Cardiovasc. Pathol. 33 (2018) 45–54, doi:10.1016/j.carpath.2018.01.003.

[4] J.J. Zheng, X. G., H.C. Wang, Y. Yan, H.Y. Wang, Clinical and histopathological analysis of 66 cases with cardiac myxoma, Asian Pac. J. Cancer Prev. 14 (2013) 1743–1746.

[5] F Fernandes, et al., Primary neoplasms of the heart. Clinical and histological presentation of 50 cases, Arq. Bras. Cardiol. 76 (2001) 231–237, doi:10.1590/s0066-782x2001000300006.

[6] S Jana, et al., Disparate remodeling of the extracellular matrix and proteoglycans in failing pediatric versus adult hearts, J. Am. Heart Assoc. 7 (2018) e010427, doi:10.1161/JAHA.118.010427.

[7] S.S Sakamuri, et al., Differential impact of mechanical unloading on structural and nonstructural components of the extracellular matrix in advanced human heart failure, Transl. Res. 172 (2016) 30–44, doi:10.1016/j.trsl.2016.02.006.

[8] N Parajuli, et al., Determinants of ventricular arrhythmias in human explanted hearts with dilated cardiomyopathy, Eur. J. Clin. Investig. 45 (2015) 1286–1296, doi:10.1111/eci.12549.

[9] S Hatami, et al., Immunity and stress responses are induced during ex situ heart perfusion, Circ. Heart Fail. (2020) CIRCHEARTFAILURE119006552, doi:10.1161/CIRCHEARTFAILURE.119.006552.

[10] Y. Imai, T. T., K. Maemura, N. Takeda, T. Harada, T. Nojiri, D. Kawanami, K. Monzen, D. Hayashi, Y. Murakawa, M. Ohno, Y. Hirata, T. Yamazaki, S. Takamoto, R. Nagai, Genetic analysis in a patient with recurrent cardiac myxoma and endocrinopathy, Circ. J. 69 (2005) 994–995.

[11] A.N.S. Roy, M. Radin, D. Sarabi, E. Shaoulian, Familial recurrent atrial myxoma: carney's complex, Clin. Cardiol. 34 (2011) 83–86.

[12] K. Wei, H. G., S.Y. Fan, X.G. Sun, S.S. Hu, Clinical features and surgical results of cardiac myxoma in Carney complex, J. Card. Surg. 34 (2019) 14–19, doi:10.1111/jocs.13980.

[13] D. Wilkes, K. C., C.T Basson, Inherited disposition to cardiac myxoma development, Nat. Rev. Cancer 6 (2006) 157–165, doi:10.1038/nrc1798.

[14] Y. Li, Z. P., Y. Ji, M. Sheppard, D.J. Jeffries, L.C. Archard, H. Zhang, Herpes simplex virus Type 1 infection associated with atrial myxoma, Am. J. Pathol. 163 (2003) 2407–2412, doi:10.1016/S0002-9440(10)63595-X.

[15] I.S. Pateras, K. E., K. Tsimaratou, M. Liontos, S. Sakellariou, T. Barlogiannis, P. Karakitsos, A. Papalois, A. Kotsinas, V.G. Gorgoulis, Detection of herplex simplex virus-1 and -2 in cardiac myxomas, J. Biomed. Biotechnol. 2012 (2012) 823949, doi:10.1155/2012/823949.

[16] M.S. Anvari, M. S., H. Goodarzynejad, S. Ziaei, M.A. Boroumand, L. Pourgholi, Y. Jenab, K. Abbasi, Association between herpes simplex virus Types 1 and 2 with cardiac myxoma, Cardiovasc. Pathol. 27 (2017) 31–34, doi:10.1016/j.carpath.2016.12.004.

[17] U.P. Schurr, D. B., B. Bode, O. Dzemali, M.Y. Emmert, M. Genoni, No association between herpes simplex virus 1 and cardiac myxoma, Swiss Med. Wkly. 141 (2011) w13223, doi:10.4414/smw.2011.13223.

[18] C. Tataroğlu, S. K., F. Döger, N. Çetin, C Ceyhan, Glandular cardiacmyxomawith associated human papilloma virus infection: case report, Turkiye Klinikleri Cardiovas. Sci. 25 (2013) 99–104.

[19] J. Yan, D. L., F. Zhang, J. He, S. Yao, X. Luo, F. Xu, Y. Chen, L. Fu, J. Xu, Y. Liu, Diffuse large B cell lymphoma associated with chronic inflammation arising within atrial myxoma: aggressive histological features but indolent clinical behaviour, Histopathology 71 (2017) 951–959, doi:10.1111/his.13336.

[20] A. Svec, M. R., M. Giles, R. Jaksa, K.A McAulay, EBV+ diffuse large B-cell lymphoma arising within atrial myxoma. An example of a distinct primary cardiac EBV+ DLBCL of immunocompetent patients, Pathol. Res. Pract. 208 (2012) 172–176, doi:10.1016/j.prp.2011.12.001.

[21] U. Tapan, J. P., J.C. Lee, A. Lerner, Epstein-Barr virus-associated diffuse large B-cell lymphoma arising in atrial myxoma: a proposal for a modified therapeutic approach, Leuk. Lymphoma 56 (2015) 505–507, doi:10.3109/10428194.2014.919632.

[22] D.F. Boyer, P.A. McKelvie, L. de Leval, K.L. Edlefsen, Y.H. Ko, Z.A. Aberman, A.E. Kovach, A. Masih, H.T. Nishino, L.M. Weiss, A.K. Meeker, V. Nardi, M. Palisoc, L. Shao, S. Pittaluga, J.A. Ferry, N.L. Harris, AR Sohani, Fibrin-associated EBV-positive large B-cell lymphoma: an indolent neoplasm with features distinct from diffuse large B-cell lymphoma associated with chronic inflammation, Am. J. Surg. Pathol. 41 (2017) 299–312, doi:10.1097/PAS.0000000000000775.

[23] G. Bartoloni, P. A., A. Giorlandino, M. Berretta, C. Mignosa, F. Italia, A. Carbone, V. Canzonieri, Incidental Epstein-Barr virus associated atypical lymphoid proliferation arising in a left atrial myxoma: a case of long survival without any postsurgical treatment and review of the literature, Cardiovasc. Pathol. 22 (2013) e5–10, doi:10.1016/j.carpath.2012.08.002.

[24] M. Fukayama, T. I., Y. Hayashi, T. Ooba, M. Koike, S. Mizutani, Epstein-Barr virus in pyothorax-associated pleural lymphoma, Am. J. Pathol. 143 (1993) 1044–1049.

[25] F. Loong, A. C., B.C. Ho, Y.P. Chau, H.Y. Lee, W. Cheuk, W.K. Yuen, W.S. Ng, H.L. Cheung, J.K. Chan, Diffuse large B-cell lymphoma associated with chronic inflammation as an incidental finding and new clinical scenarios, Mod. Pathol. 23 (2010) 493–501, doi:10.1038/modpathol.2009.168.

[26] A Orlandi, et al., Increased expression and activity of matrix metalloproteinases characterize embolic cardiac myxomas, Am. J. Pathol 166 (2005) 1619–1628, doi:10.1016/S0002-9440(10)62472-8.

[27] K.S. Mylonas, I.A. Ziogas, D.V. Avgerinos, Microenvironment in cardiac tumor development: what lies beyond the event horizon, Adv. Exp. Med. Biol. 1226 (2020) 51–56, doi:10.1007/978-3-030-36214-0_4.

[28] M. Vara-Perez, B. F.-A., P. Agostinis, Mitophagy in cancer: a tale of adaptation, Cells 8 (2019) E493, doi:10.3390/cells8050493.

[29] B. Janji, G. B., S. Chouaib, Targeting autophagy in the tumor microenvironment: new challenges and opportunities for regulating tumor immunity, Front. Immunol. 9 (2018) 887, doi:10.3389/fimmu.2018.00887.

[30] M. Wang, J. Z., L. Zhang, F. Wei, Y. Lian, Y. Wu, Z. Gong, S. Zhang, J. Zhou, K. Cao, X. Li, W. Xiong, G. Li, Z. Zeng, C. Guo, Role of tumor microenvironment in tumorigenesis, J. Cancer 8 (2017) 761–773, doi:10.7150/jca.17648.

[31] H. Folkerts, S. H., E. Vellenga, E. Bremer, V.R. Wiersma, The multifaceted role of autophagy in cancer and the microenvironment, Med. Res. Rev. 39 (2019) 517–560, doi:10.1002/med.21531.

[32] E. Koustas, P. S., G. Kyriakopoulou, A.G. Papavassiliou, M.V. Karamouzis, The interplay of autophagy and tumor microenvironment in colorectal cancer-ways of enhancing immunotherapy action, Cancers 11 (2019) E533, doi:10.3390/cancers11040533.

[33] R.N. Maes H1, A.D. Garg, P. Agostinis, Autophagy: shaping the tumor microenvironment and therapeutic response, Trends Mol. Med. 19 (2013) 428–446, doi:10.1016/j.molmed.2013.04.005.

[34] B. Chiu, E. J., F. Shen, B. Chiu, C. Sergi, Autophagy-inflammasome interplay in heart failure: a systematic review on basics, pathways, and therapeutic perspectives, Ann. Clin. Lab. Sci. 47 (2017) 243–252.

[35] I. Dikic, Z. Elazar, Mechanism and medical implications of mammalian autophagy, Nat. Rev. Mol. Cell Biol. 19 (2018) 349–364, doi:10.1038/s41580-018-0003-4.

[36] L.B. Frankel, M. L., A.H Lund, Emerging connections between RNA and autophagy, Autophagy 12 (2017) 3–23, doi:10.1080/15548627.2016.1222992.

[37] B. Levine, G. Kroemer, Biological functions of autophagy genes: a disease perspective, Cell 176 (2019) 11–42, doi:10.1016/j.cell.2018.09.048.

[38] R.C. Russell, H.X. Yuan, K. G., Autophagy regulation by nutrient signaling, Cell Res. 24 (2014) 42–57, doi:10.1038/cr.2013.166.

[39] C. Tukaj, The significance of macroautophagy in health and disease, Folia Morphol. 72 (2013) 87–93.

[40] B. Adam, B. A., K.M. Dominy, E. Chapman, R. Gill, L.G. Hidalgo, C. Roufosse, B. Sis, M. Mengel, Multiplexed color-coded probe-based gene expression assessment for clinical molecular diagnostics in formalin-fixed paraffin-embedded human renal allograft tissue, Clin. Transpl. 30 (2016) 295–305, doi:10.1111/ctr.12689.

[41] H. Armanious, B. Adam, D. Meunier, K. Formenti, I. Izevbaye, Digital gene expression analysis might aid in the diagnosis of thyroid cancer, Curr. Oncol. 27 (2020) e93–e99, doi:10.3747/co.27.5533.

[42] Y. Okazaki, S. Y., S. Kitada, I. Matsunaga, E. Nogami, T. Watanabe, Y. Sasaguri, Y. Honma, T. Itou, Significance of 18 F-FDG PET and immunohistochemical GLUT-1 expression for cardiac myxoma, Diagn. Pathol. 9 (2014) 117 111-114, doi:10.1186/1746-1596-9-117.

[43] S. Tsuyuki, M. T., M. Kawazu, K. Kudo, A. Watanabe, Y. Nagata, Y. Kusama, K. Yoshida, Detection of WIPI1 mRNA as an indicator of autophagosome formation, Autophagy 10 (2014) 497–513, doi:10.4161/auto.27419.

[44] B. Chiu, E. Jantuan, F. Shen, B. Chiu, C. Sergi, Autophagy-inflammasome interplay in heart failure: a systematic review on basics, pathways, and therapeutic perspectives, Ann. Clin. Lab. Sci. 47 (2017) 243–252.

[45] D.J. Klionsky, B. S., Dynamic regulation of macroautophagy by distinctive ubiquitin-like proteins, Nat. Struct. Mol. Biol. 21 (2014) 336–345.

[46] R. Mathew, C. K., B. Beaudoin, N. Vuong, G. Chen, H.Y. Chen, K. Bray, A. Reddy, G. Bhanot, C. Gelinas, R.S. Dipaola, V. Karantza-Wadsworth, E. White, Autophagy suppresses tumorigenesis through elimination of p62, Cell 137 (2009) 1062–1075, doi:10.1016/j.cell.2009.03.048.

[47] R. Mathew, S. K., B. Beaudoin, C.M. Karp, K. Bray, K. Degenhardt, G. Chen, S. Jin, E. White, Autophagy suppresses tumor progression by limiting chromosomal instability, Genes Dev. 21 (2007) 1367–1381, doi:10.1101/gad.1545107.

[48] M Alipour, et al., A balanced IL-1beta activity is required for host response to citrobacter rodentium infection, PLoS One 8 (2013) e80656, doi:10.1371/journal.pone.0080656.

[49] C.M. Sergi, B. Chiu, Targeting NLRP3 inflammasome in an animal model for Coronavirus Disease 2019 (COVID-19) caused by the Severe Acute Respiratory Syndrome Coronavirus 2 (SARS-CoV-2), J. Med. Virol. (2020), doi:10.1002/jmv.26461.